Pergamon

0301-9322(94)E0027-G

Int. J. Multiphase Flow Vol. 20, No. 5, pp. 957–967, 1994

0301-9322/94 $7.00 + 0.00

AN INVISCID INVESTIGATION OF THE INITIATION OF ROLL WAVES IN HORIZONTAL GAS–LIQUID FLOWS

G. BREYIANNIS[1], D. VALOUGEORGIS[1], V. BONTOZOGLOU[2] and A. GOULAS[1]

[1]Laboratory of Fluid Mechanics and Turbomachinery, Department of Mechanical Engineering, Aristotle University of Thessaloniki, 54006 Thessaloniki, Greece

[2]Laboratory of Transport Processes, Department of Mechanical Engineering, University of Thessaly, Pedion Areos, 38334 Volos, Greece

(Received 10 April 1993; in revised form 1 March 1994)

Abstract—A model with constant vorticity in the liquid phase has been applied to the study of interfacial waves between two inviscid fluids in relative motion, in order to take into account the shear induced into the liquid by the cocurrent gas flow. For a range of values of gas velocity and vorticity in the liquid phase a new wave pattern is calculated, consisting of a recirculating eddy below the wave crest. It is suggested that, under certain conditions, the onset of this new type of waves (rather than the classical Kelvin–Helmholtz instability mechanism) provides the inviscid analog to the experimentally observed transition to roll waves.

Key Words: inviscid, roll waves, constant vorticity

1. INTRODUCTION

Gas–liquid interfacial waves play a key role in a variety of flows appearing in process equipment as well as in nature. They affect the pressure drop and hold up of flow in channels and pipes and determine momentum and mass transfer in the upper ocean. Inviscid analysis has proven—within its inherent limitations—useful in describing the mechanisms of several wave-related phenomena (atomization of ripples, appearance of large waves, slugging in pipes etc.).

The classical Kelvin–Helmholtz instability theory has been of central importance in understanding these two-phase flow phenomena (Kordyban & Ranov 1970; Mishima & Ishii 1980; Andritsos & Hanratty 1987a). However, non-linear interfacial waves have been considered by relatively few investigators. An excellent review of early work in the field is provided by Miles (1986). Saffman & Yuen (1982)—by implementing a second-order analysis—found that there is a distinct factor, associated with the Kelvin–Helmholtz instability, that limits the existence of finite steady waves. Bontozoglou & Hanratty (1988) extended these results for interfacial waves between fluids of finite depth.

Lately, the assumption of constant vorticity has been incorporated (Pullin & Grimshaw 1983; Simmen & Saffman 1985; Teles da Silva & Peregrine 1988) to take into account the shear stresses generated at the interface or the bottom of the liquid layer. This model is more realistic for thin films or viscous liquids since vorticity will be distributed across the entire layer. Although linear shear strictly describes laminar flows, it has also been pointed out (Teles da Silva & Peregrine 1988) that waves riding on wind-induced drift, "see" a linear velocity profile if they are short enough. In this case, the vorticity can be satisfactorily approximated by its local value at the interface. Recent results (Breyiannis *et al.* 1993) in the above context, showed that for negative vorticity (wind-induced shear) a new regime is present, where interfacial gravity waves develop a recirculating eddy at the crest. This flow pattern appears at high enough gas velocities but still well below the Kelvin–Helmholtz limit. It is suggested that these waves are the inviscid analog of what is described in the experimental literature as "roll waves".

Over the past years, there have been numerous reports of roll waves in gas–liquid flows, the term being used (in a rather loose sense) to describe flow surges in the liquid layer which differ from the classical Stokes waves, both in appearance and in properties. Such occurrences have been

reported for horizontal gas–liquid flows at high enough gas velocities (Hanratty & Hershman 1961; Miya *et al.* 1971; Bruno & McCready 1988) and also for vertical free-falling films with or without shear (Telles & Dukler 1970; Brauner *et al.* 1985; Karapantsios *et al.* 1989). It is noted that in both cases roll waves are associated with high vorticity in the liquid layer, imposed, for horizontal flows, by the gas shear and for vertical films by the action of gravity.

Attempts to explain and model this flow regime include computation of the flow field below a wave in free-falling films (Brauner 1989), using as input the wave shape and celerity. This computation demonstrates that a large mixing eddy exists in the wave core. Of particular interest to the present study is the work of Andritsos & Hanratty (1987a), where it is indicated that the appearance of roll waves in horizontal pipe flow can be predicted by an inviscid Kelvin–Helmholtz analysis. It is also worth noting, that, some time ago the possibility of roll wave formation in ocean flows has been suggested (Banner & Phillips, 1974). Namely, it was argued that when the flow near the surface is rotational, the appearance of a stagnation point near the wave crest—which is considered a mechanism for incipient breaking—should not necessarily be connected with a discontinuity in surface slope (geometrical limit). However, to the best of our knowledge, there has been, up to now, no direct theoretical computation of roll waves starting from first principles.

In the present work, the results of Breyiannis *et al.* (1993) are extended and applied to a two-phase flow situation of practical interest. In particular, the theory is extended to include in its formulation the effect of surface tension and simple analytical criteria (derived from linear and weakly non-linear analyses) are presented for the onset of inviscid roll waves and compared with previously obtained numerical results. The analysis is subsequently applied to liquid films thin enough that the gas-induced shear is linear. The relation between gas velocity and liquid vorticity (both treated as independent parameters in formal inviscid theory) is modeled through a stress balance and use of an expression for the friction factor at the interface. It is demonstrated that, under such conditions, the incipient appearance of roll waves (predicted from theory) seems more relevant to the experimentally observed transition than the classical Kelvin–Helmholtz instability.

The formulation of the problem is presented in section 2, supplemented by a linear analysis. Weakly non-linear waves are discussed in section 3, where the validity of the second-order analysis is established. In section 4 the results for the aforementioned flow conditions are derived, while in section 5 the conclusions are given.

2. PROBLEM FORMULATION AND LINEAR ANALYSIS

The flow configuration under consideration is sketched in figure 1, where both a physical reference frame and a reference frame with the wave at rest are depicted. The interface is located at $y = \eta(x)$ while the top and bottom boundaries are at d_2 and $-d_1$ respectively. The origin is chosen so that the mean elevation $\overline{\eta(x)}$ over one wavelength is zero. Properties of the lower fluid are denoted by subscript 1 and those of the upper fluid by subscript 2. The two fluids are assumed to be stably stratified by gravity so $\rho_2 < \rho_1$ and the upper fluid is moving relative to the lower one with a horizontal velocity U. The undisturbed flow of the lower fluid is a shear flow with velocity that varies linearly in the vertical direction. The liquid shear is described by a vorticity vector, whose magnitude is specified by ζ and whose direction is perpendicular to the (x, y) plane. The upper flow is assumed to be irrotational and both fluids are taken as incompressible and inviscid. The flow shown in figure 1 corresponds to $\zeta < 0$, with the wave propagating downstream. This flow configuration is equivalent to a shear flow generated by the wind.

Inviscid flows with initially uniform vorticity distribution are ammenable to simplified analysis because Kelvin's circulation theorem guarantees that the vorticity will always remain constant. It is this feature of constant vorticity flows that simplifies the analysis. Poisson's equation,

$$\nabla^2 \Psi = -\zeta. \qquad [1]$$

holds within the fluid and Ψ can be written as the sum of a particular solution satisfing [1] (for $\zeta = \text{const.}$ this is simply the original flow field) and an irrotational stream function $\Psi(x, y)$.

Therefore, the velocity field can be described by a superposition of an irrotational component to the original linear shear. The two components of the velocity vector are defined by

$$\mathbf{u}_1 = \left(\frac{\partial \phi_1}{\partial x} - \zeta y, \frac{\partial \phi_1}{\partial y}\right) \qquad [2]$$

and

$$\mathbf{u}_2 = \left(\frac{\partial \phi_2}{\partial x}, \frac{\partial \phi_2}{\partial y}\right),$$

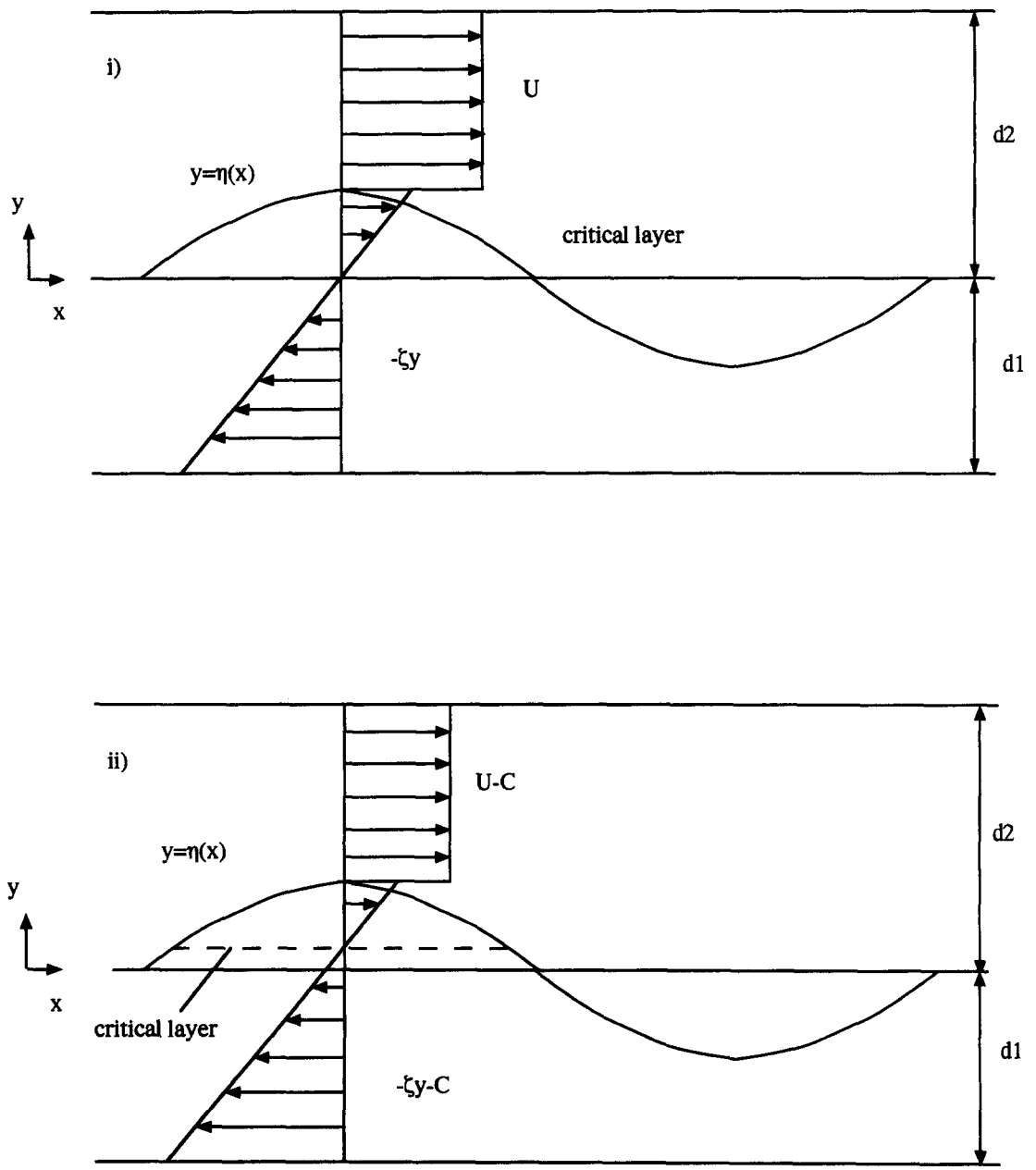

Figure 1. Sketch of the flow configuration for wave propagating downstream, $\zeta < 0$, (i) physical reference frame; (ii) reference frame moving with the wave phase velocity.

where the velocity potentials ϕ_i, $i = 1, 2$, satisfy Laplace's equation $\nabla^2\phi_i = 0$ in each fluid domain. The dynamical condition of equal pressures on the interface is presented in the form of a combined Bernoulli equation at $y = \eta$,

$$\frac{1}{2}\left(\left(\frac{\partial\phi_1}{\partial x} - \zeta y - C\right)^2 + \left(\frac{\partial\phi_1}{\partial y}\right)^2\right) - \frac{1}{2}r\left(\left(\frac{\partial\phi_2}{\partial x} - C\right)^2 + \left(\frac{\partial\phi_2}{\partial y}\right)^2\right) + (1-r)g\eta - \sigma\frac{\dfrac{\partial^2\eta}{\partial^2 x}}{\left(1+\left(\dfrac{\partial\eta}{\partial x}\right)^2\right)^{3/2}} + K = 0. \quad [3]$$

Equation [3] is given in a reference frame moving with the wave celerity, thus rendering the wave motionless.

It is noted that for uniform vorticity, ζ, the Bernoulli constant is modified to read $K_1 = K_1 + \zeta\psi$, where ψ is the local value of the stream function (Batchelor 1983). In this case the Bernoulli equation is applied on the interface which is a streamline of the motion ($\psi = \text{const.}$) and the additional term is incorporated in the constant K of [3].

The leading order terms for the wave profile and the volocity potentials are

$$\eta(w) = \alpha\cos w, \quad [4]$$

$$\phi_1(x, y, t) = A_1(e^{ky} + e^{-2kd_1}e^{-ky})\sin w, \quad [5]$$

and

$$\phi_2(x, y, t) = Ux + B_1(e^{ky} + e^{2kd_2}e^{-ky})\sin w, \quad [6]$$

where α is half the wave height ($H = 2\alpha$), $w = kx - \omega t$ is the wave phase, $A_1 = C_l\alpha/(1-X)$, $B_1 = -(U - C_1)\alpha/(1 - Y^{-1})$ with C_l being the linear wave phase speed and X, Y defined as $X = e^{-2kd_1}$, $Y = e^{-2kd_2}$.

Linear analysis provides a first insight into the characteristics of waves with constant vorticity. The linearized solution of the problem is readily found and gives a dispersion relation which can be written as

$$\frac{1+X}{1-X}C_l^2 + r\frac{1+Y}{1-Y}(U - C_l)^2 = \frac{g}{k}(1-r) + \frac{C_l}{k}\zeta + \frac{\sigma k}{\rho_1}, \quad [7]$$

where g is the gravitational acceleration, $k = 2\pi/L$ is the wave number with L representing the wave length, r is the density ratio ρ_2/ρ_1 and σ is the surface tension. The critical current velocity corresponding to the linear Kelvin–Helmholtz limit, U_{cl}, is derived from [7] as

$$U_{cl} = u_d + \left[u_d^2 + \frac{(g/k(1-r) + \sigma k/\rho_1)(X' + rY') + (X'u_d)^2}{rX'Y'}\right]^{1/2}, \quad [8]$$

where

$$X' = \frac{1+X}{1-X} \quad Y' = \frac{1+Y}{1-Y} \quad u_d = \frac{\zeta}{2kX'}.$$

As it is seen from [8], the linear Kelvin–Helmholtz limit depends on the vorticity of the lower fluid. Although the minimum U_{cl} is reached at slightly negative vorticity, large negative vorticities cause the dynamical limit to move to larger current velocities.

It has been shown by Breyiannis *et al.* (1993) that, in the moving reference frame, inviscid roll waves are characterized by a closed eddy below the crest. The recirculating eddy is first manifested by the appearance of a stagnation point on the wave crest when the x-component of the lower fluid velocity equals the wave celerity. This limiting condition will be applied, to first order, in the linear expression for the liquid velocity, to calculate a minimum necessary amplitude for the transition to occur. It is evident that linear theory may no longer be valid for such amplitudes. However, the prediction may prove reasonably accurate. Similar reasoning for the prediction of the geometrical limit of Stokes waves has been used in the engineering literature (Mishima & Ishii 1980) with relative success.

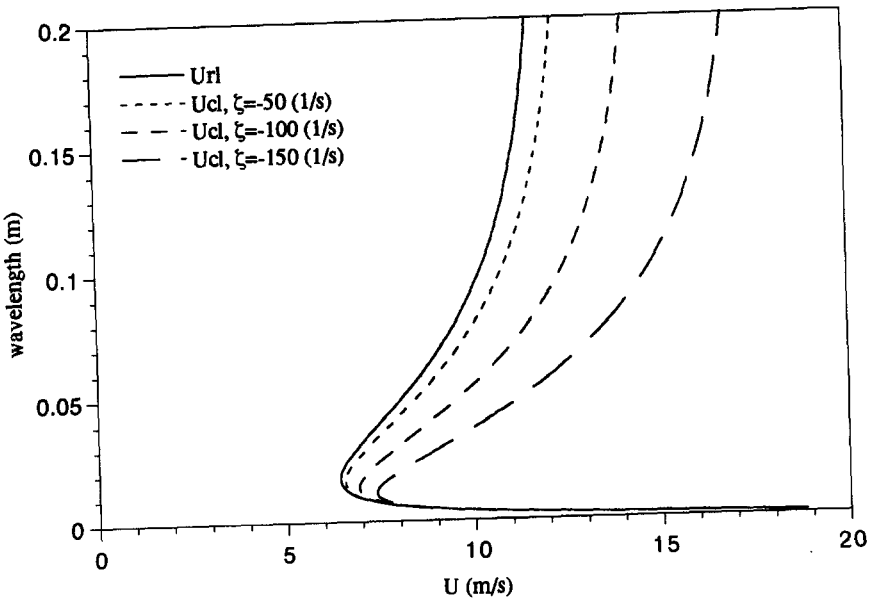

Figure 2. The U_{rl} and the U_{cl} for various vorticities versus the wavelength for air–water flow with $r = 0.0013$, $d_2 = 0.02$, $d_1 = 0.002$ m and $\sigma = 0.073$ (N/m).

The x-velocity component of the lower fluid at the interface [2] is found from the velocity potential [5] to be,

$$u_x = \left(k \frac{C_l}{1 - X} (e^{k\eta} + X e^{-k\eta}) - \zeta \right) \alpha \cos w. \qquad [9]$$

with C_l defined from the linear dispersion relation [7]. The stagnation point first appears at the crest ($w = 0$) when u_x becomes equal to the phase velocity. Setting $u_x(x = 0) = C_l$ in [9], the following linear estimate of the critical roll wave amplitude is found.

$$\alpha_r = \frac{C_l}{X' k C_l - \zeta}. \qquad [10]$$

In the following section this is compared with numerical and weakly non-linear results.

As the amplitude of the wave increases beyond this point, a critical layer is created, originating from two symmetric stagnation points at some distance along the profile. The position of the critical layer changes depending on the wave celerity. In particular, the critical layer is located over the mean level for $C > 0$ and below the mean level for $C < 0$, as is clarified by observing the flow field in figure 1. Thus, for $C > 0$ the appearance of a recirculating eddy is possible only for finite amplitude waves, while in the case of $C < 0$ the eddy may occur even for linear waves. It is seen that the limiting case of a linear wave is retained when $C_l = 0$. By setting $C_l = 0$ in [7] the corresponding current velocity

$$U_{rl} = \left[\frac{g(1 - r)/k + \sigma k/\rho_1}{r} \frac{1 - Y}{1 + Y} \right]^{1/2} \qquad [11]$$

is obtained, which we define as the critical "roll velocity". For $U > U_{rl}$ all waves will present the new flow pattern.

It is noted that the condition $u_x - C_l = 0$ can be satisfied for positive C_l also, for some values of the vorticity ζ, if the perturbed flow is superimposed. However since the term on the right-hand side of [9] is of the order of α, the wave celerity must also be of the order of α. Thus from the linear point of view the criterion ($C_l = 0$) is acceptable.

In figure 2, the critical roll velocity U_{rl} and the critical linear velocity U_{cl} are plotted versus the wave length for various values of vorticity, keeping constant the values of the depths and the density ratio. It is clear that the present inviscid roll wave approach predicts a possible initation of roll

waves ahead of the classical Kelvin–Helmholtz theory. The difference between the onset of linear roll waves and Kelvin–Helmholtz instability is particularly pronounced for longer waves. It increases drastically with the magnitude of liquid shear and it is significant even at the minimum wavelength. The above results provide only a first approach to the problem since, as is discussed in the following section, non-linearity greatly affects the transition by causing the waves to roll at even smaller current velocities. In that sense, roll waves depend significantly on the value of vorticity.

3. NON-LINEAR ROLL WAVES

A complete description of the analysis for non-linear waves has been presented in previous work (Breyiannis *et al.* 1993). In this work, similar analysis has been undertaken but with the added feature of the inclusion of the surface tension term. The following expression for the wave celerity has been derived:

$$C=\frac{rY'U+\zeta/[2k]}{X'+rY'}+\sqrt{\left(\frac{rY'U+\zeta/[2k]}{X'+rY'}\right)^2-\frac{rY'U^2-g(1-r)/k-\sigma k/\rho_1-\alpha^2\Delta}{X'+rY'}}. \qquad [12]$$

where α is the wave amplitude and Δ the non-linear term

$$\begin{aligned}\Delta=&\tfrac{1}{2}k^2\left(\lambda^2\frac{1+X}{1-X}\left(1-4\frac{X}{(1-X)^2}\right)+r(U-\lambda)^2\frac{1+Y}{1-Y}\left(1-4\frac{Y}{(1-Y)^2}\right)\right)\\&+2k\left(\lambda\zeta\frac{X}{(1-X)^2}\right)-\frac{1}{4}\left(\zeta^2\frac{1+X^2}{1-X^2}\right)-\frac{3}{8}\frac{\sigma k^3}{\rho_1}\\&+\tfrac{1}{2}k^2\frac{\left(\lambda^2\dfrac{1+4X+X^2}{(1-X)^2}-r(U-\lambda)^2\dfrac{1+4Y+Y^2}{(1-Y)^2}-\dfrac{2}{k}\left(\lambda\zeta\dfrac{1+X^2+X}{1-X^2}\right)+\dfrac{\zeta^2}{2k^2}\right)^2}{\left(\lambda^2\dfrac{1-X}{1+X}+r(U-\lambda)^2\dfrac{1-Y}{1+Y}-3\dfrac{\sigma k}{\rho_1}\right)}.\end{aligned} \qquad [13]$$

The above expression reduces, for $\zeta=0$, to that given by Miles (1986).

Equation [12] and the corresponding second-order velocity potential is used to evaluate the transition to roll waves through the already familiar criterion,

$$\frac{\partial\phi_1}{\partial x}-\zeta y-C=0.$$

The U velocity that satisfies the above criterion is defined as the roll velocity U_r. In figure 3 the effect of wave amplitude and vorticity on U_r, for a representative case of gravity waves ($\sigma=0$) is given. A direct comparison between the above expressions and the fully non-linear numerical results provided by a boundary integral code (Breyiannis *et al.* 1993) is also made. These results are presented in the form of dimensionless quantities. All lengths are non-dimensionalized with the wavenumber k and the velocities are Froude numbers using k^{-1} as characteristic length. The reader should refer to the original publication for more details on the implemented numerical scheme.

Weakly non-linear results follow closely the numerical ones up to the point where higher harmonics appear in the wave profile. This point is considered to be the limit of validity of the second-order analysis. The linear relation [10] is in good agreement with numerical results for large values of ζ and small wave amplitude. Its most serious drawback though is that, unlike the second-order theory, it does not predict the leveling off of the numerical results, observed at higher wave amplitudes.

An interesting point in figure 3 is that the appearance of roll waves is a subcritical phenomenon, in the sense that, for finite amplitude waves, the transition occurs at lower gas velocities. The variation in the transition gas velocity with increasing height is certainly significant, with reductions of the order of 50% being manifested for waves with intermediate height. Thus, finite amplitude effects play a key role and cannot be accounted for by a small correction.

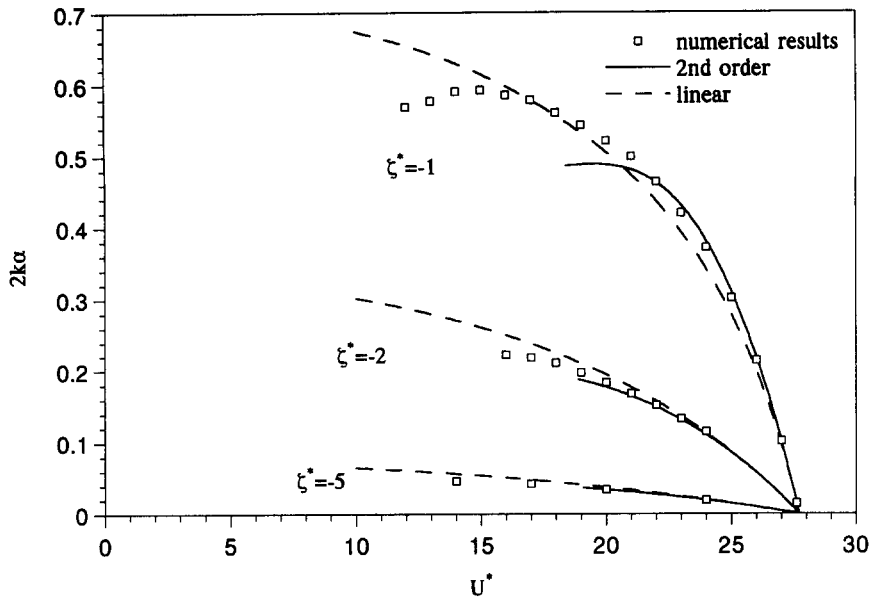

Figure 3. Effect of vorticity on the transition to roll waves for gravity air–water waves. Comparison between several schemes. $r = 0.0013$, $e^{-kd_2} = 0$, $e^{kd_1} = 0.25$, $\zeta^* = \zeta/\tau/\sqrt{gk}$ and $U^* = U/\sqrt{g/k}$

An increase in the magnitude of vorticity of the liquid, for constant gas velocity, is seen to reduce the wave height required for transition. However, according to an important finding of the constant vorticity model (Telles da Silva & Peregrine 1988), the maximum wave height also decreases with increasing vorticity. Thus, the behavior of U_r is quite complex. A roll wave can appear at small current velocities, either when a wave increases in height or when the fluid becomes more sheared. The above arguments, in connection with the assumption that α scales with depth, could suggest that, for high liquid Re_L numbers, it is the wave amplitude that controls the appearance of roll waves while for small Re_L it is the liquid shear.

Figure 4 depicts the effect of surface tension for a given small wavelength. A convenient scale has been invoked to obtain information about the behavior of waves of small wavelength. The

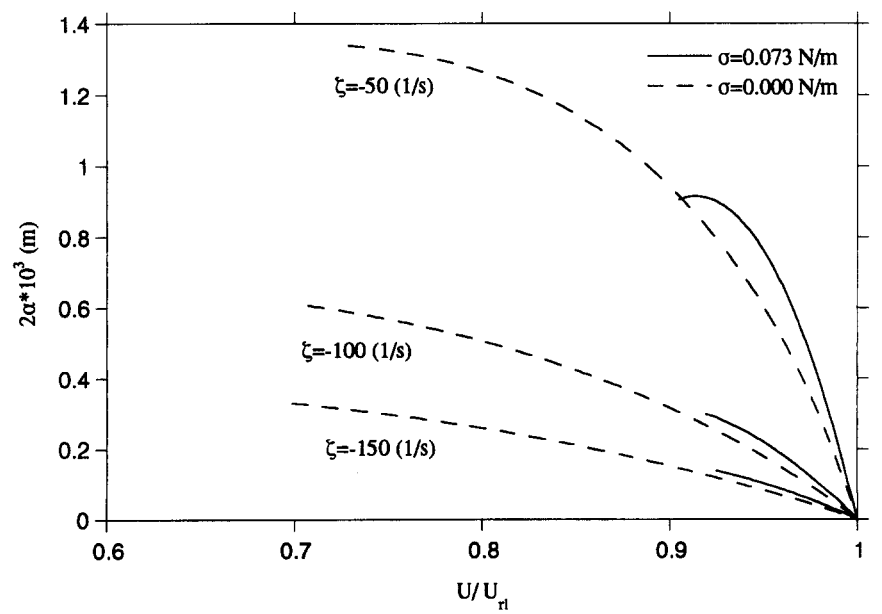

Figure 4. The transition to roll waves for air–water flow and various vorticities. Effect of surface tension. $r = 0.0013$, $d_2 = 0.02$ m, $d_1 = 0.002$ m and $L = 0.03$ m.

depths are chosen to have a ratio of $d_1/d_2 = 0.1$, representative of a typical cocurrent, stratified flow. Surface tension seems to delay the appearance of roll waves not only in absolute but in relative values as well. In the weakly non-linear analysis higher harmonics appear sooner when surface tension is present, although the pattern is the same and U_r is a strong function of the wave amplitude and vorticity. This appearance, however, does not necessarily indicate the limit of validity of second-order theory, as double-crested capillary-gravity waves are known to exist (Bontozoglou & Hanratty 1990).

The theoretical information gathered up to this point is used in the next section to analyse a representative flow with linear velocity profile, that of a film in laminar motion (high viscocity or very thin film). As noted in the introduction, this is the most straightforward but not the only case where a constant vorticity model is applicable.

4. PREDICTION OF ROLL WAVES

Inviscid theory treats gas velocity and liquid vorticity as independent input parameters. However, when the vorticity of the liquid is induced through shear, gas velocity and vorticity are related. To estimate the vorticity induced by the superimposed gas flow on a laminar liquid film, the following expression for the gas friction factor (Andreussi *et al.* 1985) is used:

$$f_s = 0.046 \mathrm{Re}_G^{-0.2} \qquad [14]$$

The interfacial shear stress is then calculated to be equal to

$$\tau_s = 0.023 \rho_2 \nu_2^{0.2} U^{1.8} d_2^{-0.2}. \qquad [15]$$

A more accurate estimate should include the effect of interfacial waves (as in Andritsos & Hanratty 1987b). Another simplification—implicit in the above formulation of the friciton factor—is the neglect of the liquid velocity in comparison with the much higher gas velocity. Given the preliminary nature of our results, neither of the above elaborations was deemed necessary.

For a laminar film, the constant vorticity imposed by a gas shear is given by

$$\zeta = \frac{\tau_s}{\mu_1}. \qquad [16]$$

Equation [16] is plotted in figure 5 (solid line) for the flow of air over water [figure 5(a)] and over a 50% water–glycerol mixture [figure 5(b)]. Also plotted are the predictions of inviscid theory for the onset of Kelvin–Helmholtz instability [8] and for the incipient appearance of roll waves [10] for three representative wave lengths. Transition is predicted to take place at the value of vorticity corresponding to the intersection of each of the inviscid curves with [16]. It is easier to envision this, if it is considered that increasing the gas velocity is equivalent to moving along the solid line [16].

What becomes immediately evident from figure 5(a) is that, for a laminar water film, Kelvin–Helmholtz instability should never take place. This has to do with the fact that the critical velocity U_{cl} is a strong increasing function of the magnitude of vorticity $|\zeta|$. Therefore, increasing the gas velocity does not guarantee an approach to Kelvin–Helmholtz instability, as higher values of U lead also to an increase in $|\zeta|$. The transition to roll waves, however, is not very sensitive to vorticity and such waves should appear. It is an interesting coincidence that the gas velocity for the transition, U_r, is roughly equal to the Kelvin–Helmholtz instability velocity for $\zeta = 0$.

Finally, for the viscous case [figure 5(b)] it is observed that although both roll waves and Kelvin–Helmholtz waves may appear, the significance of Kelvin–Helmholtz instability is restricted to short waves, whereas longer roll waves are possible.

5. CONCLUDING REMARKS

A constant liquid–vorticity model has been applied to describe interfacial waves in horizontal gas–liquid flows. For high gas velocity and liquid vorticity, waves comprising a recirculating eddy at the crest are calculated. Linear and weakly non-linear approximations compare reasonably well

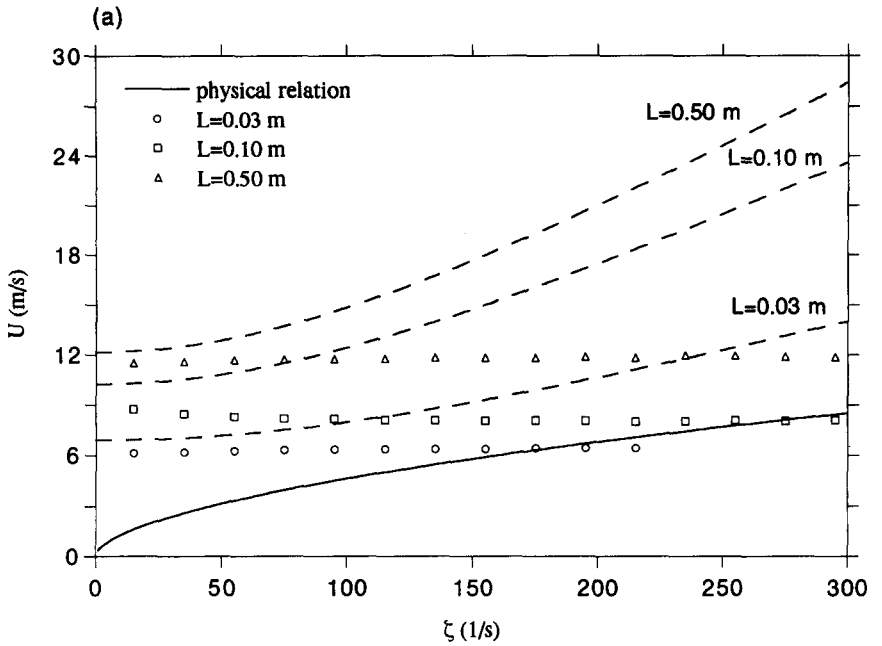

Figure 5(a). Comparison between the predictions of K–H theory (dashed lines), roll waves theory (discrete points) and a physical relation for air–water flow with $r = 0.0013$, $d_2 = 0.02$ m, $d_1 = 0.002$ m and $\sigma = 0.073$ (N/m).

with numerical results and indicate a strong dependence of the transition to roll waves on wave amplitude.

It is shown that the new flow pattern always appears at lower gas velocities than the Kelvin–Helmholtz instability, the difference between the two velocities being more pronounced for longer waves and higher vorticity. In fact, a detailed calculation valid for laminar liquid flow,

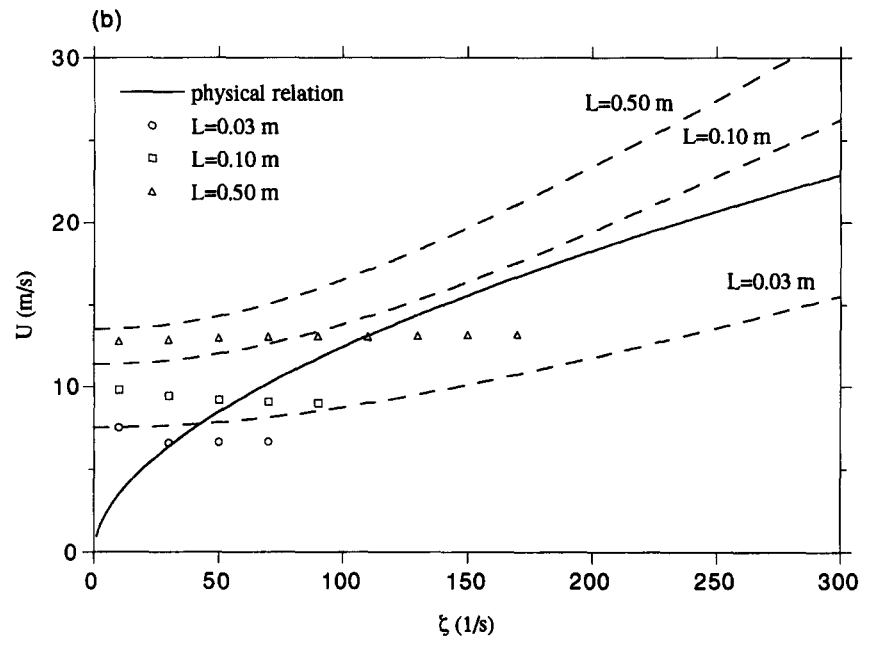

Figure 5(b). Comparison between the predictions of K–H theory (dashed lines), roll waves theory (discrete points) and a physical relation for air–50% water/glycerol mixture flow with $r = 0.00105$, $d_2 = 0.02$ m, $d_1 = 0.002$, m, $\sigma = 0.069$ (N/m) and $\mu_1 = 6$ cP.

indicates that Kelvin–Helmholtz instability is generally limited to short waves and may not be realized for thin films of liquids with low viscocity.

A different behavior is expected when the liquid film is turbulent. The liquid velocity gradient at the interface will, for the same gas velocity, be less steep than in laminar flow, resulting in smaller values of vorticity. Thus, Kelvin–Helmholtz instability is expected to play a more active role. It should be noted, however, that the non-uniformity of vorticity across a turbulent layer makes the present analysis valid only for short waves.

Finally, it should be stressed that the present results refer to steady-progressive waves of permanent form and do not address the stability question. The situation is similar to the classical water wave theory, which, though incapable of predicting the growth mechanism, does describe satisfactorily the characteristics of waves once they have formed. In the present case, the formation of roll waves at gas velocities below the Kelvin–Helmholtz limit could be attributed to energy input through gas-pressure variations in phase with the wave slope (Miles 1957). These considerations, however, are beyond the scope of the present work.

REFERENCES

ANDREUSSI, P., ASALI, J. C. & HANRATTY, T. J. 1985 Initiation of roll waves in gas–liquid flows. *AIChE Jl* **31,** 119–126.

ANDRITSOS, N. & HANRATTY, T. J. 1987a Interfacial instabilities for horizontal gas–liquid flows in pipelines. *Int. J. Multiphase Flow* **13,** 583–603.

ANDRITSOS, N. & HANRATTY, T. J. 1987b Influence of interfacial waves in stratified gas–liquid flows. *AIChE Jl* **33,** 444–454.

BANNER, M. L. & PHILLIPS, O. M. 1974 On the incipient breaking of small scale waves. *J. Fluid Mech.* **65,** 647–656.

BATCHELOR, G. K. 1983 *An Introduction to Fluid Dynamics.* Cambridge University Press, Cambridge, MA.

BONTOZOGLOU, V. & HANRATTY, T. J. 1988 Effects of finite depth and current velocity on large amplitude Kelvin–Helmholtz waves. *J. Fluid Mech.* **196,** 187–204.

BONTOZOGLOU, V. & HANRATTY, T. J. 1990 Capillary-gravity Kelvin–Helmholtz waves close to resonance. *J. Fluid Mech.* **217,** 71–91.

BRAUNER, N. 1989 Modelling of wavy flow in turbulent free falling films. *Int. J. Multiphase Flow* **15,** 505–520.

BRAUNER, N., MOALEM MARON, D. & DUKLER, A. E. 1985 Modelling of wavy flow in inclined thin films in the presence of interfacial shear. *Chem. Engng Sci.* **40,** 923–937.

BREYIANNIS, G., BONTOZOGLOU, V., VALOUGEORGIS, D. & GOULAS, A. 1993 Large amplitude interfacial waves on a linear shear flow in the presence of a current. *J. Fluid Mech.* **249,** 499–519.

BRUNO, K. & MCCREADY, M. J. 1988 Origin of roll waves in horizontal gas–liquid flows. *AIChE Jl.* **34,** 1431–1440.

HANRATTY, T. J. & HERSHMAN, A. 1961 Initiation of roll waves. *AIChE Jl* **7,** 488–497.

KARAPANTSIOS, T. D., PARAS, S. V. & KARABELAS, A. J. 1989 Statistical characteristics of free falling films at high Reynolds numbers. *Int. J. Multiphase Flow* **15,** 1–21.

KORDYBAN, E. S. & RANOV, T. 1970 Mechanism of slug formation in horizontal two-phase flow. *J. Basic Engng* **92,** 857–864.

MILES, J. W. 1957 On the generation of surface waves by shear flows. *J. Fluid Mech.* **3,** 185–204.

MILES, J. W. 1986 Weakly nonlinear Kelvin–Helmholtz waves. *J. Fluid Mech.* **172,** 513–529.

MISHIMA, K. & ISHII, M. 1980 Theoretical prediction of onset of horizontal slug flow. *ASME J. Fluids Engng ASME Trans.* **102,** 441–445.

MIYA, M., WOODMANSEE, D. E. & HANRATTY, T. J. 1971 A model for roll waves in gas–liquid flow. *Chem. Engng Sci.* **26,** 1915–1931.

PULLIN, D. I. & GRIMSHAW, R. H. J. 1983 Interfacial progressive gravity waves in a two-layer shear flow. *Phys. Fluids* **26,** 1731–1739.

SAFFMAN, P. G. & YUEN, H. C. 1982 Finite-amplitude interfacial waves in the presence of a current. *J. Fluid Mech.* **123,** 459–476.

SIMMEN, J. A. & SAFFMAN, P. G. 1985 Steady deep-water waves on a linear shear current. *Stud. Appl. Math.* **73,** 35–57.

TELES, A. S. & DUKLER, A. E. 1970 Statistical characteristics of thin, vertical, wavy liquid films. *Ind. Engng Chem. Fundam.* **9,** 412–421.

TELES DA SILVA, A. F. & PEREGRINE, D. H. 1988 Steep, steady surface waves on water of finite depth with constant vorticity. *J. Fluid Mech.* **195,** 281–302.